Progress In Electromagnetics Research, Vol. 129, 365–385, 2012

WIDEBAND CIRCULARLY POLARIZED UHF RFID READER ANTENNA WITH HIGH GAIN AND WIDE AXIAL RATIO BEAMWIDTHS

P. Wang[1, 2, *], G. Wen[1], J. Li[1], Y. Huang[1], L. Yang[1], and Q. Zhang[1]

[1]Centre for RFIC and System Technology, School of Communication and Information Engineering, University of Electronic Science and Technology of China, Chengdu 611731, China

[2]Department of Electronic Engineering, College of Electronic and Information Engineering, Chongqing Three Gorges University, Chongqing 404000, China

Abstract—A broadband circularly polarized patch antenna with high gain and wide axial ratio beamwidths is proposed for ultra-high-frequency (UHF) RF identification (RFID) applications in this paper. The antenna is composed of a square patch, a feed network printed on the bottom side of the substrates and an antenna radome. The CP radiation of the proposed antenna is excited by four cylinder probes which transmit four signals that have equal amplitude with quadrature phase difference (0°, 90°, 180°, and 270°) generated from the feed network. To obtain an optimum peak gain and a broad CP bandwidth, 100 Ω isolation resistor is omitted in the feed network for obtaining high radiation efficiency, and the effects of varying the feed positions and dimensions of the various parameters on the antenna performances are respectively investigated. Simulation results are compared with the measurements, and a good agreement is obtained. The measured results show that the proposed antenna can provide broad impendence bandwidth of 19.7% (815–993 MHz) (reflection coefficient less than −15 dB), a maximum gain of 9.65 dBi, and a 3-dB axial ratio (AR) bandwidth of about 11% (860–960 MHz). The results indicate that the proposed antenna is an excellent candidate for UHF RFID reader system. At last, read performance of the proposed antenna array in RFID systems is presented, which verify the superior features of the proposed antenna in practical RFID system applications.

Received 25 April 2012, Accepted 7 June 2012, Scheduled 26 June 2012

* Corresponding author: Ping Wang (wangpingcqz@163.com).

1. INTRODUCTION

Currently, radio frequency identification (RFID) system in the ultra-high-frequency (UHF) bands (840–960 MHz) has received considerable attention for various commercial applications, such as automatic retail item management, warehouse management, access control system, electronic toll collection, and etc. [1–4]. This is because the UHF band can provide high data transfer rate and broad readable range. However, the UHF frequencies authorized for RFID applications are different in different countries and regions [5], e.g., 840.5–844.5 MHz and 920.5–924.5 MHz in China, 866–869 MHz in Europe, 902–928 MHz band in North and South of America, 866–869 MHz and 920–925 MHz in Singapore, and 952–955 MHz in Japan, and so on. Thus, the requirement for a universal UHF RFID reader include: enough wide bands to cover all UHF RFID frequencies ranges, perfect performance and lost cost. An RFID system generally consists of a reader, a tag and a data processing system. The RFID reader antenna is one of the important components in RFID systems and its capability will determine the performance of whole RFID system. In order to obtain well read performance, the reader antenna need to be designed for circular polarization (CP), because circularly polarized antennas can increase orientation diversity and reduce the loss caused by the multi-path effects between the reader and the tag antenna. General speaking, circular polarization commonly needs two orthogonal linear polarizations with a 90° phase shift. CP antennas can be categorized into two types: single-fed type and multi-fed type.

A typical example for single-fed circularly polarized antenna is a rectangle or circular patch by trimming opposite corners or edge of metallic patch and selecting suitable feed position [6–9], others are cutting slots on radiation patch [6, 10–19]. However, these antennas have inherent narrow impedance and axial ratio (AR) bandwidth (typically 1%–4%). Commonly one used method to achieve wide AR bandwidths is the use of parasitic elements [20–28]. In [20], the author used the probe-fed rectangle patch and added an almost square parasitic element to achieve a 13% axial ratio bandwidth of less than 2.5 dB. Chung and Mohan presented a systematic design method to obtain 3-dB AR bandwidth of 8% in C band and 17.3% in Ku band by introducing a coupled patch above radiation patch [21]. In [22], two mixed structures (i.e., a solid patch and a ring) were used for further enhancing the bandwidth of 18.85%. In [5, 23–25], the authors investigated the cut-corner stacked patch antenna carefully with different feed method, where 3-dB axial ratio (AR) bandwidths of about 16.4%, 20.2%, 13.5% and 11% respectively can be achieved.

Nevertheless, most of these antennas either have large antenna height or narrow impedance bandwidths (the antenna reflection coefficient less than -15 dB), which may not suitable for practical applications. As we know, the coupling feed technique including slot coupling [29–33] and L-shaped strip coupling [34–38] has wide bandwidths. However, the aperture coupled patch antenna needs a reflecting plate to block back radiation, which increases the complexity of the antenna configuration. In addition, the effects of the length of the vertical and horizontal portion of the L-shaped strip on input resistance and reactance are dependent, which result in complex design process. In [29, 30], the authors also added a parasitic triangular or circular patch to produce another resonance frequency bands, and consequently the CP bandwidth is further enhanced, whereas the antennas have also large height of antenna.

It is commonly known that multi-feed circularly polarized antenna have wider bandwidths than single-fed structure, so many researchers are proposed to design hybrid feed network with a relative phase shift of 90 degree and equal amplitude [39–46]. In [39, 40], Wilkinson power dividers with 100 Ω isolation resistor were used to achieve wide impedance bandwidths and AR bandwidths, whereas leads to low radiation efficiency due to large insertion loss [42]. It is important to note that a stacked annular-ring antenna with a novel divider formed by the shape of Archimedes gradual-change lines at the inside of the annular ring was proposed for RFID applications [42]. However, the antenna cannot provide deep resonant characteristics. In [44], Lau et al. presented a rotated CP patch array fed by a divider for RFID smart bookshelf applications, whereas the voltage standing-wave ratio (VSWR) of the antennas is only less than 2 in the 3-dB AR bands, and the antenna also provides unsatisfactory lowest AR values, which is not suitable for the RFID reader requiring good impedance matching (VSWR < 1.5).

This article presents a four-feed patch antenna with wide beamwidths and high gain for RFID systems. This antenna is composed of a square patch, a feed network printed on the bottom side of the substrates and an antenna radome. The radiating square patch is fed by the feed network with equal amplitude and quadrature phase difference (0°, 90°, 180°, and 270°). A parametric study showing the impact of the various parameters on the antenna performance is presented and both simulated and measured results are given in this article.

2. ANTENNA CONFIGURATION

The geometry of the proposed antenna is shown in Fig. 1. In this design, the center frequency of antenna is chosen as $f_0 = 915\,\text{MHz}$ ($\lambda = 327.9\,\text{mm}$). The antenna is composed of an aluminum radiating plate of 0.5 mm thick, a PCB substrate, a feed network, a coaxial cable and four metallic cylinder probes, four hollow medium cylinders 1, four hollow medium cylinders 2, an antenna radome and an aluminum ground plane of 2 mm thick. The radiating plate is a square patch with dimensions of $128\,\text{mm} \times 128\,\text{mm}$ ($\sim 0.3904\lambda \times 0.3904\lambda$), which is supported by using four hollow substrate cylinders 2, with length of h_1 and dielectric constant 2.1, above a thin dielectric layer: 1.54 mm thick Arlon AD320 (relative permittivity $\varepsilon_r = 3.2$, $\tan\delta = 0.003$), and is fed by four cylinder probes through hollow substrate cylinders 2.

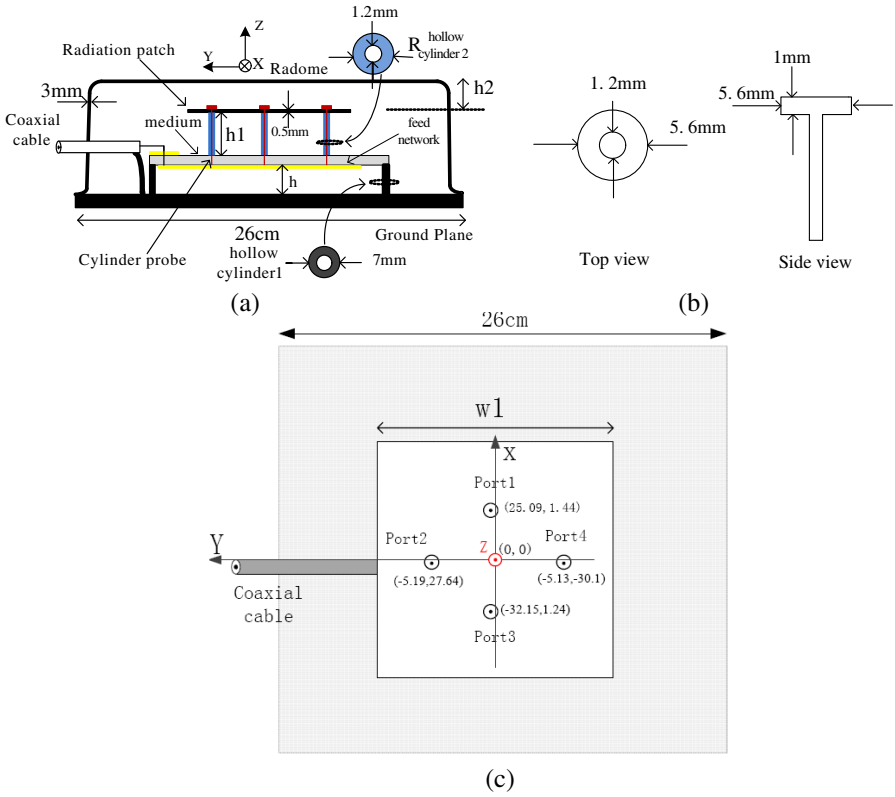

Figure 1. Configuration of the proposed antenna. (a) Side view. (b) Geometry of cylinder probe. (c) Top view (Dimensions in mm).

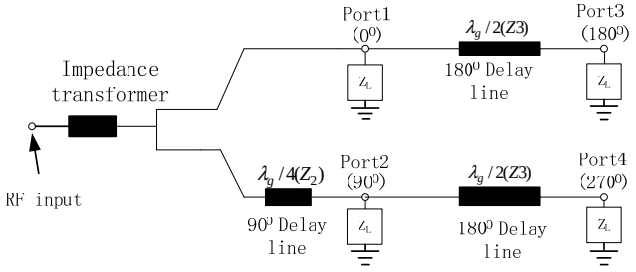

(a)

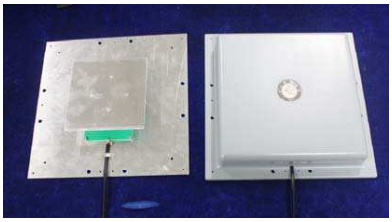

(b)

Figure 2. (a) Equivalent-circuit model of the feed network. (b) Antenna prototype.

The probes are of diameter of 1.2 mm, and transmit four signals that have equal amplitude with quadrature phase difference (0°, 90°, 180°, and 270°) generated from the feed network. In our design, mechanism of every probe-feed radiating patch is similar with the technique of common coaxial probe-feed patch antenna [6], thus all of the probes need to be connected to about 50 Ω microstrip-line, in succession to about 100 Ω microstrip-line, ultimately by a stepped impedance transformer to a 50 Ω coaxial cable. As shown in Fig. 1(a), the feed network is printed on the bottom side of PCB dielectric layer, which is placed over the ground plane with a distance h and is fixed by using four metallic screws via four hollow medium cylinders 1. An antenna radome of 3 mm thick fabricated by ABS medium (relative permittivity $\varepsilon_r = 2.8$, $\tan\delta = 0.01$) is used to cover the whole antenna in order to protect the antenna from damage. The coaxial cable extends through the antenna radome (ABS medium) and the inner conductor of that is directly soldered to the feed network, whereas the outer conductor is connected the ground plane.

The feed network is composed by a stepped impedance transformer, 90° delay line, and 180° delay lines as shown in Fig. 2(a), and brings into sequential rotation of current on the radiation patch for CP radiation. To avoid low radiation efficiency, 100 Ω isolation

resistor is omitted in the feed network. By properly selecting the positions of four feed points and carefully optimizing the stepped impedance transformer, the input resistance and reactance can be easily controlled to achieve a wide impedance bandwidth. The other designed parameters are eventually determined with $h = 1\,\text{mm}$, $h_1 = 25\,\text{mm}$, $h_2 = 6.5\,\text{mm}$, $w_1 = 128\,\text{mm}$, $R = 2.4\,\text{mm}$. With aid of simulation by the Ansoft HFSS 13 3-D EM simulator, which is based on the finite-element method (FEM), the antenna is optimized and then prototyped. A photograph of the fabricated antenna with circularly polarized characteristic is shown in Fig. 2(b).

3. SIMULATED AND MEASURED RESULTS

The antenna was measured in an anechoic chamber using the NSI300V-30X30 far-field measurement system and Agilent N5230A series vector

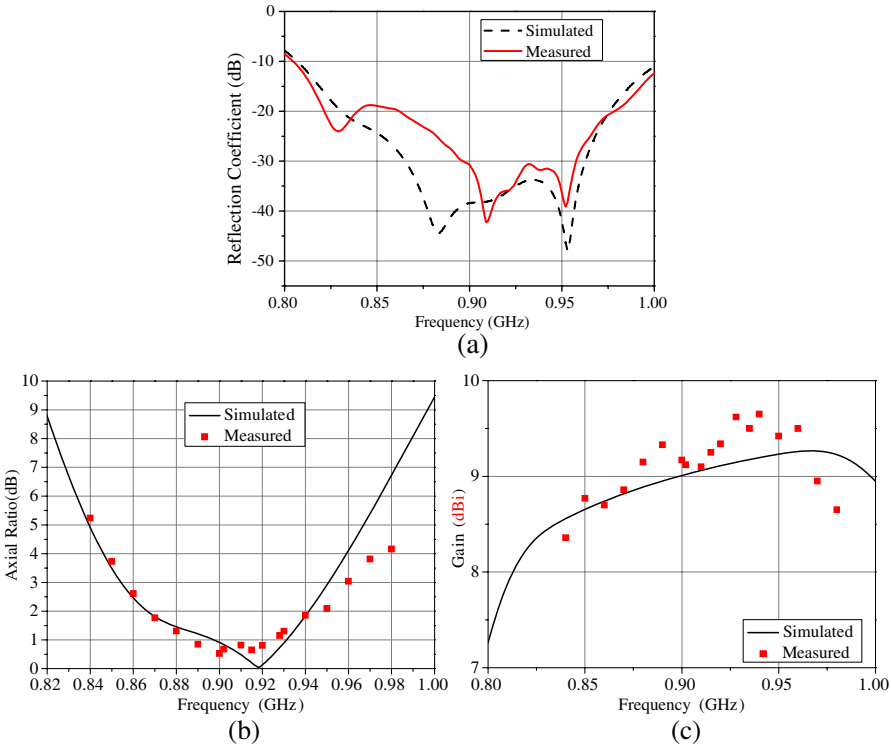

Figure 3. Simulated and measured results of the proposed antenna. (a) Reflection coefficient. (b) AR. (c) Gain.

network analyzer. Measured and simulated results for the proposed antenna are shown in Fig. 3, which shows good agreement. It is observed from Fig. 3(a) that the measured reflection coefficient is less than −15 dB over the frequency ranges of 815–993 MHz (19.7%), which can easily cover the entire UHF RFID frequency band of 860–960 MHz. Fig. 3(b) shows the comparison between the simulated and measured AR at broadside direction ($+z$). The measured 3-dB AR bandwidth of 860–960 MHz or 11% is obtained. Within the frequency range, the measured gain of the proposed antenna is 9.26 dBi on average and 9.65 dBi at maximum when the operating frequency is 940 MHz. A stable gain over the operating band is found experimentally.

Figure 4 shows the comparison between the simulated and measured radiation patterns at 870, 915, and 950 MHz, in the xz-plane and yz-plane, respectively, which shows good agreement. It is seen that the proposed antenna has a symmetrical radiation pattern across

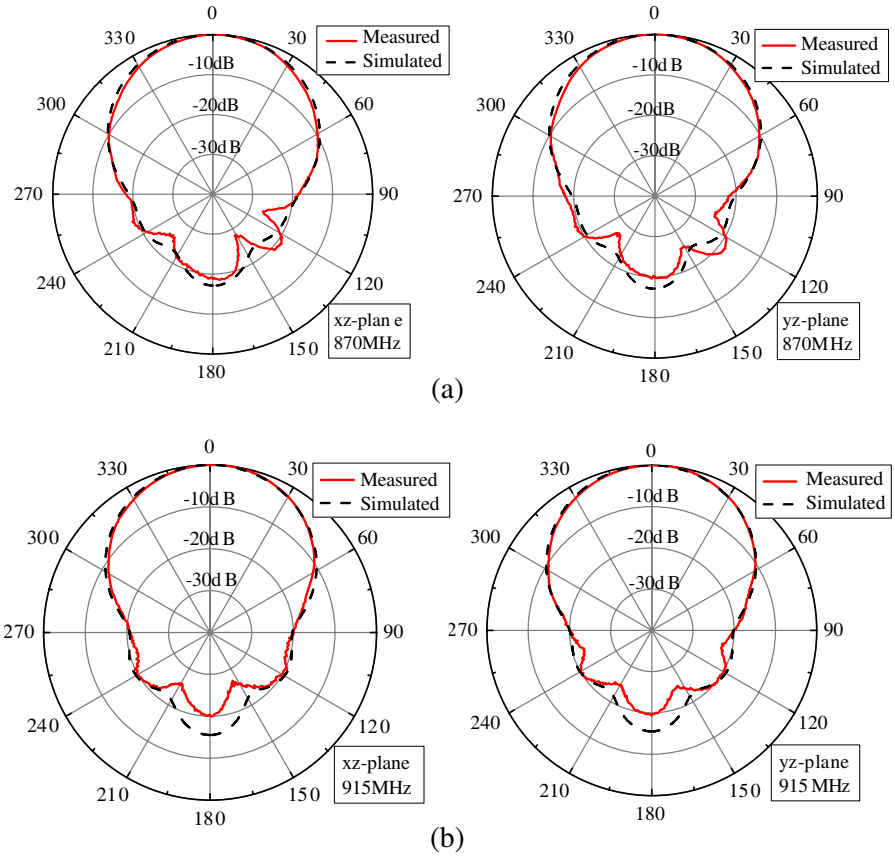

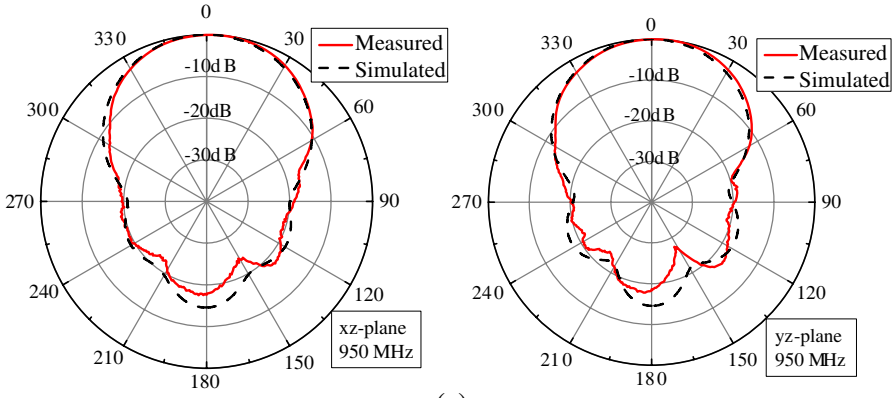

(c)

Figure 4. Simulated and measured radiation patterns of the proposed antenna. (a) 870 MHz. (b) 915 MHz. (c) 950 MHz.

Table 1. Summary of the radiation characteristics.

Frequency (MHz)	Half Power Beamwidth		3 dB AR Beamwidth	
	xz-plane	yz-plane	xz-plane	yz-plane
860	61.6°	61.8°	72°	75°
902	60.2°	59.5°	97°	112°
915	61.4°	60.4°	85°	117°
928	60.9°	59.3°	89°	105.5°
950	61°	61.5°	88.5°	102.5°

the operating bandwidth and its maximum beam is always directed to the $+z$-axial direction, which have great advantages in practical applications. It is also observed that the measured 3 dB beamwidth of the antenna prototype is more than 60°, and the measured front-to-back ratio is better than 17.6 dB at all measured frequencies. The half-power beamwidth and 3-dB AR beamwidth of the antenna prototype at some measured frequencies are summarized in Table 1. The half-power beamwidths are about 60 degree in the xz-plane and in the yz-plane. Results in Table 1 show that the half-power beamwidths are stable in both xz-plane and yz-plane within the operating bandwidths. In addition, the AR is less than 3 dB within the half-power beamwidth, although the 3-dB AR beamwidths are different in the xz- and yz-planes.

4. PARAMETRIC STUDIES

In this section, CP radiation mechanism and parametric studies of the proposed antenna are presented to provide more detailed information about the antenna design and optimization. The parameters under study include the height of PCB substrate, height of radiating patch, size of radiating patch, height of antenna radome, and diameter of hollow cylinder 2. To better understand the influence of the parameters on the performance of the antenna, only one parameter at a time will be varied, while others are kept unchanged unless especially indicated.

4.1. Mechanism of CP Radiation

As shown in Fig. 5, the electric field of a wave traveling in $+z$-direction consists of four linearly polarized components in x- and y-direction. As a function of time and position, these electric field components in x- and y-directions are given by

$$E_1 = E_{10}\sin(\omega t - \beta z) \quad (1)$$

$$E_2 = E_{20}\sin(\omega t - \beta z + \varphi) \quad (2)$$

$$E_3 = E_{30}\sin(\omega t - \beta z + 180) \quad (3)$$

$$E_4 = E_{40}\sin(\omega t - \beta z + \varphi + 180) \quad (4)$$

where E_{10}, E_{20}, E_{30}, E_{40} are, respectively, the maximum magnitudes of four electric field components, the quantity φ is the phase difference of the electric fields E_1 and E_2 or E_3 and E_4. So

$$\vec{E} = \vec{E}_1+\vec{E}_2+\vec{E}_3+\vec{E}_4 = E_{10}\sin(\omega t-\beta z)\widehat{x}+E_{20}\sin(\omega t-\beta z+\varphi)\widehat{y} - E_{30}\sin(\omega t - \beta z + 180)\widehat{x} - E_{40}\sin(\omega t - \beta z + \varphi + 180)\widehat{y} \quad (5)$$

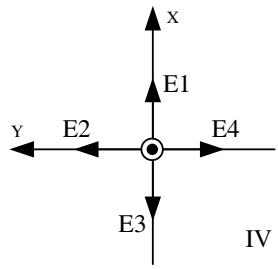

Figure 5. Distribution of the linearly polarized waves.

At $z = 0$, we have

$$\begin{aligned}\vec{E} &= [E_{10}\sin\omega t - E_{30}\sin(\omega t + 180)]\widehat{x} \\ &\quad + [-E_{40}\sin(\omega t + \varphi + 180) + E_{20}\sin(\omega t + \varphi]\widehat{y} \\ &= (E_{10} + E_{30})\sin(\omega t)\widehat{x} + (E_{20} + E_{40})\sin(\omega t + \varphi)\widehat{y} \end{aligned} \quad (6)$$

Circular polarization can be achieved only when the magnitudes of the two components are the same and the time-phase difference between them is odd multiples of $\pi/2$. That is

$$|E_x| = |E_y| \Rightarrow E_{10} + E_{30} = E_{20} + E_{40}$$

$$\Delta\phi = \varphi = \begin{cases} +\left(\dfrac{1}{2} + 2n\right)\pi, n = 0, 1, 2, \ldots, \\ \text{right circularly polarized waves,} \\ -\left(\dfrac{1}{2} + 2n\right)\pi, n = 0, 1, 2, \ldots, \\ \text{left circularly polarized waves,} \end{cases}$$

From Eqs. (6), one founds

$$\begin{aligned} \sin^2(\omega t) &= \frac{E_x^2}{(E_{10}+E_{30})^2} \\ \cos^2(\omega t) &= \pm\frac{E_y^2}{(E_{20}+E_{40})^2} \end{aligned} \quad (7)$$

By eliminating the ωt, we obtain $\frac{E_x^2}{(E_{10}+E_{30})^2} \pm \frac{E_y^2}{(E_{20}+E_{40})^2} = 1$, corresponding to right and left circularly polarized waves, respectively.

To further perceive why the CP can be generated by the designed antenna, we can examine how the surface current distribution in the radiating patch varies with time. Shown in Fig. 6 are the proposed antenna's current distributions at 915 MHz (simulated also

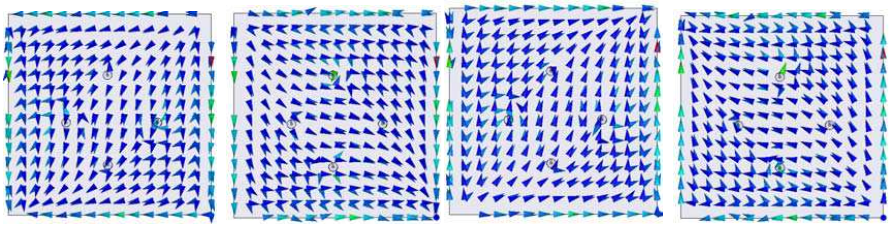

(a) (b) (c) (d)

Figure 6. Simulated instantaneous current distributions on the radiating patch for the proposed RFID antenna at $f = 915$ MHz. (a) $\varphi = 0°$. (b) $\varphi = 45°$. (c) $\varphi = 90°$. (d) $\varphi = 135°$.

using Ansoft HFSS) for four different time instants, i.e., $\omega t = 0°$, 90°, 180°, and 270°. At $\omega t = 0°$, the end point of surface currents is 45° with respect to the $+y$ axis. The surface current distribution at $\omega t = 180°$ (270°) is just opposite to that at $\omega t = 0°$ (90°). The surface current distribution varying as a function of time in such a fashion would result in revolving phenomenon, that is, the current flows turning the x-axis into y-axis like a right-handed circularly polarized (RHCP) wave. Note that the surface currents at other frequencies within the 3-dB AR band are varied as functions of time also in a similar manner, and hence are not shown here for brevity.

4.2. Height of PCB Substrate (h)

Figure 7 shows the antenna performance curves for different values of h: 0.6 mm, 1 mm, 1.5 mm, 2 mm, and 3 mm. It is clearly observed that

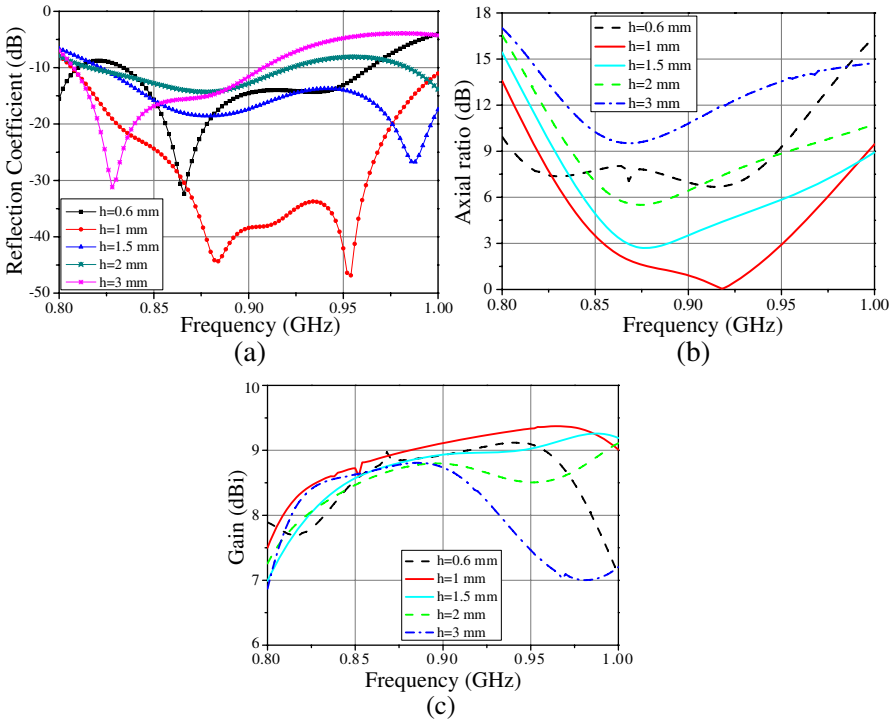

Figure 7. Effect of height of PCB substrate (h) on the antenna performance. (a) Reflection coefficient. (b) AR at broadside direction ($+z$). (c) Gain.

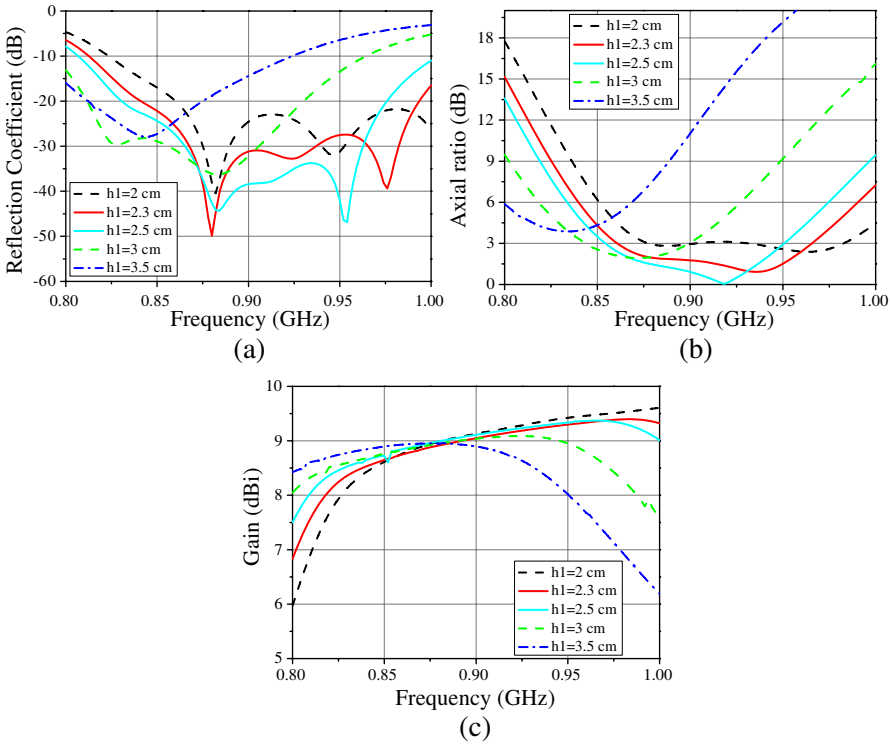

Figure 8. Effect of height of radiating patch (h_1) on the antenna performance. (a) Reflection coefficient. (b) AR at broadside direction ($+z$). (c) Gain.

the variety of the height of substrate board have a significant effect on the reflection coefficient, AR and gain of the antenna. As the figure describes, decreasing h causes better impedance matching and wider 3 dB AR bands, and higher gain values. However, over decreasing of h (such as $h = 0.6$ mm) will degrade the antenna performance. Results have revealed that the best performance is obtained when $h = 1$ mm.

4.3. Height of radiating patch (h_1)

The effect of varying the height (h_1) of radiating patch on the reflection coefficient, AR and gain of the antenna is shown in Fig. 8. The figure shows that with increasing h_1 from 2 cm to 3.5 cm, the resonance bandwidth is gradually shifted downward. This is owing to the current path is extended as the height h_1 increases. Furthermore, when over increasing of h_1 (such as exceed 2.5 cm) will result in no enough

operational bandwidth to cover UHF RFID bands (860–960 MHz). It is seen from previous study that the height of radiating patch has a significant effect on antenna performance. Hence, to have a wider and proper bandwidth, the height of radiating patch need to be well optimized and the extracted optimum parameter value is $h_1 = 25$ cm

4.4. Size of Radiating Patch (w_1)

In this part of parametric study, we change w_1 to show effects of variation in radiating patch dimensions on the antenna performance Fig. 9 exhibits the simulation results for various values when other parameters are kept unchanged. It is found that the effect of w_1 on antenna performance is similar with that of h_1 The results show that by increasing w_1, the figure shows various shapes for the five different radiating patch sizes. To have a wider 3 dB AR bandwidth, the size of

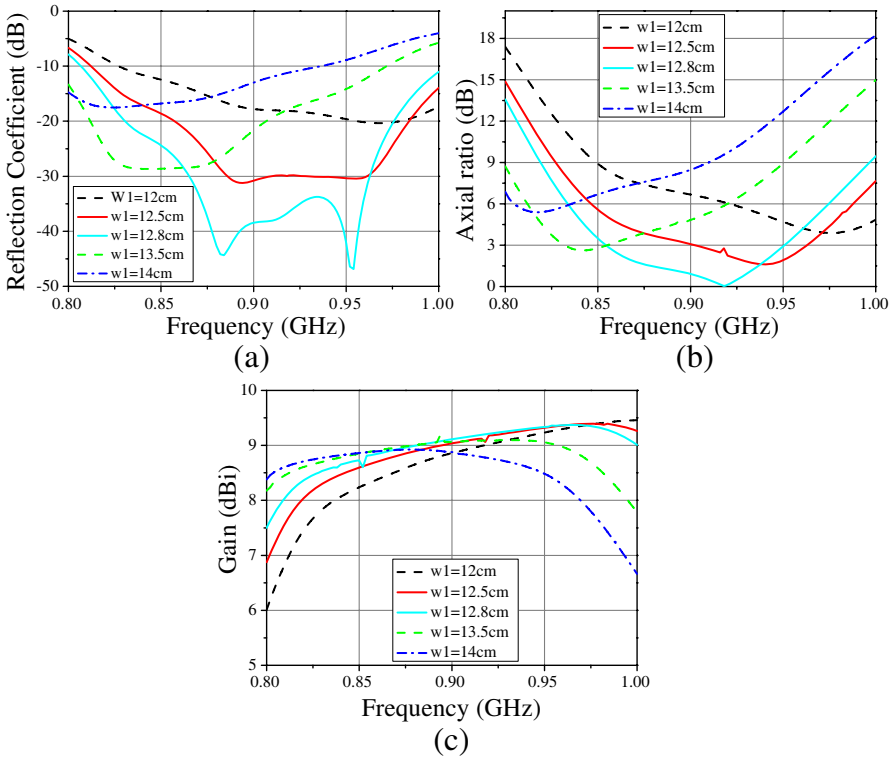

Figure 9. Effect of length of radiating patch (w_1) on the antenna performance. (a) Reflection coefficient. (b) AR at broadside direction ($+z$). (c) Gain.

radiating patch (w_1) needs to be well optimized. Results have revealed that the best performance is obtained when $w_1 = 12.8\,\text{cm}$.

4.5. Height of Antenna Radome (h_2)

The effect of the height h_2 of antenna radome on reflection coefficient and gain of the antenna is illustrated in Fig. 10. It is clearly known from the figure that with decreasing h_2, the 3 dB AR bandwidth increase and the resonance band is shifted downward, and vice versa. The results show that by decreasing h_2, the 3 dB AR bandwidth of the antenna will be improved and a lowest AR value which is close to 0 dB can be obtained. To have a wider and proper AR bandwidth, height of antenna radome (h_2) also needs to be well optimized. Results have revealed that the best performance is obtained when $h_2 = 0.65\,\text{cm}$.

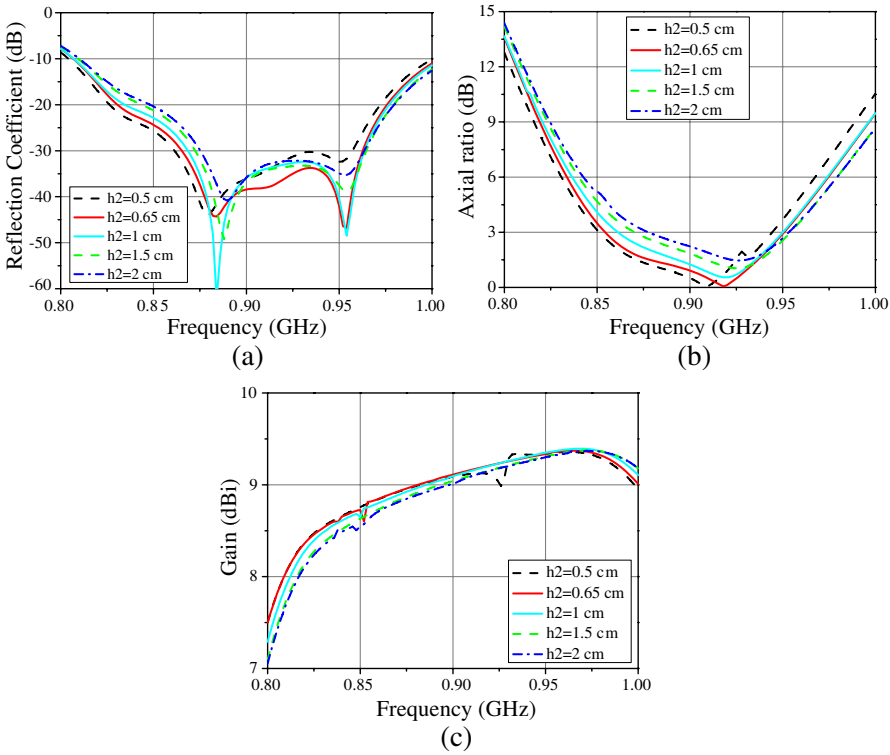

Figure 10. Effect of distance between top side of radome and radiating patch (h_2) on the antenna performance. (a) Reflection coefficient. (b) AR at broadside direction ($+z$). (c) Gain.

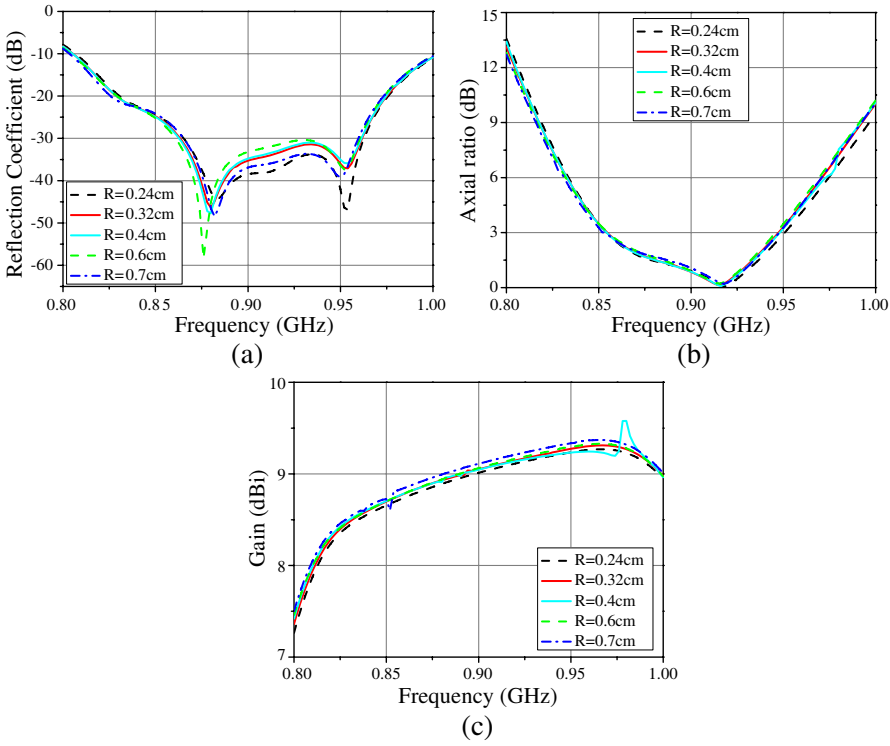

Figure 11. Effect of diameter of hollow cylinder $2(R)$ on the antenna performance. (a) Reflection coefficient. (b) AR at broadside direction $(+z)$. (c) Gain.

4.6. Diameter of Hollow Cylinder $2(R)$

Compared to previous study parameters (h, h_1, h_2, w_1), the diameter R of hollow cylinder 2 has less effect on impedance matching, AR, and gain. As illustrated in Fig. 11, when R is increased from 0.24 cm to 0.7 cm, the AR bandwidth and gain are slightly changed. It is also observed that with increasing diameter R, the peak gain will be increased slightly. Thus, in practical design, large diameter R of hollow cylinder 2 will be used to reduce the manufacturing difficulty and the cost.

5. READ PERFORMANCE IN UHF RFID SYSTEM

To verify the superior features of the proposed antenna in practical RFID system applications, an antenna array consisted of four same

elements is used to measure the read performance of the proposed antenna. Geometrical distribution of the proposed antenna array is shown in Fig. 12. In the experiment, every antenna is connected with one port of UHF RFID reader to detect two hundred of UHF RFID tags. Two elements of the antenna array are uniformly located on the top of the metallic shelf with height of 1.35 m and width of 1.8 m, and face to the stacked tags; another two elements are symmetrically located in the profile and are directed to tags with a tilted angle. Two hundreds of invengo's tags [47] and an in-house developed reader system are used. The invengo's tags and reader systems all can operate

Table 2. Read performance of the proposed antenna array.

Read time(5s) / Antenna label	Detected Quantity						
	First Read	Second Read	3th Read	4th Read	5th Read	6th Read	average
NO.1 and NO.3	199	199	198	199	199	199	199
NO.2 and NO.4	199	198	199	199	199	198	199
All	200	200	200	200	200	200	200

Table 3. Read performance of the proposed antenna array.

Read time(2s) / Antenna label	Detected Quantity						
	First Read	Second Read	3th Read	4th Read	5th Read	6th Read	Average
NO.1 and NO.3	198	199	197	199	199	198	198
NO.2 and NO.4	198	197	198	196	198	199	197
All	199	199	200	199	199	199	199

Figure 12. Measured environment of the proposed antenna array.

at the frequency band of 860–960 MHz. In the measurement, the tags are stacked to many layers and placed on a trolley platform. The measured results are summarized in Table 2 and Table 3. Maximum output power of the reader systems is about 30 dBm. From the two tables, the proposed antenna can quickly read almost all tags within 2 seconds, and the proposed antenna array consisted of four elements within five seconds can read all tags. The performance results are important for UHF RFID systems in practical applications and also prove the outstanding CP characteristics directly.

6. CONCLUSION

A CP UHF RFID reader antenna with wide AR beamwidths and high-gain characteristics has been presented in this paper. To obtain broad bandwidths and high gain, a broadband 90° feed network without 100 Ω isolation resistor has been presented to excite the CP operation and by selecting the position of probes and adjusting each parameter carefully it is easy to obtain the optimal antenna design The optimized antenna has achieved the desired performance over the UHF RFID band of 860–960 MHz with an average gain of 9.25 dBi, AR of less than 3 dB, reflection coefficient is less than −15 dB and 3-dB AR beamwidth of larger than 72°. Finally, excellent read capability of the proposed antenna array is also illustrated, which show that the proposed antenna array can quickly read all tags within a very short time (less than 5 s). Therefore, the proposed antenna can be a good candidate for UHF RFID applications.

ACKNOWLEDGMENT

This work is supported by Research Fund for the Doctoral Program of Higher Education of China (No. 20110185110014) and also supported by Guangdong province special funds for development of new strategic emerging industries (new high-end electronic information) (No. 2011912028).

REFERENCES

1. Finkenzeller, K., *RFID Handbook*, 2nd Edition, Wiley, New York, 2003.
2. Jamlos, M. F., A. R. B. Tharek, M. R. B. Kamarudin, P. Saad, O. Abdul Aziz, and M. A. Shamsudin, "Adaptive beam steering of RLSA antenna with RFID technology," *Progress In Electromagnetics Research*, Vol. 108, 65–80, 2010.

3. Li, X. and J. Liao, "Eye-shaped segmented reader antenna for near-field UHF RFID applications," *Progress In Electromagnetics Research*, Vol. 114, 481–493, 2011.
4. Amin, Y., Q. Chen, H. Tenhunen, and L.-R. Zheng, "Performance-optimized quadrate bowtie RFID antennas for cost-effective and eco-friendly industrial applications," *Progress In Electromagnetics Research*, Vol. 126, 49–64, 2012.
5. Chen, Z. N., X. Qing, and H. L. Chung, "A universal UHF RFID reader antenna," *IEEE Trans. Microw. Theory Tech.*, Vol. 57, No. 5, 1275–1282, May 2009.
6. Lin, C. L., et al., *Antenna Engineering Handbook*, 1st Edition, Publishing House of Electronics Industry, China, 2002.
7. Kwa, H. W., X. Qing, and Z. N. Chen. "Broadband single-fed single-patch circularly polarized antenna for UHF RFID applications," *In Proc. IEEE AP-S Int. Symp.*, 1–4, San Diego, CA, 2008.
8. Chi, L. P. and S. S. Bor, "A wideband wide-strip dipole antenna for circularly polarized wave operations," *Progress In Electromagnetics Research*, Vol. 100, 69–82, 2010.
9. Tsai, C.-L., "A coplanar-strip dipole antenna for broadband circular polarization operation," *Progress In Electromagnetics Research*, Vol. 121, 141–157, 2011.
10. Nasimuddin, Z., N. Chen, and X. Qing. "Asymmetric-circular shaped slotted microstrip antennas for circular polarization and RFID applications," *IEEE Transactions on Antennas and Propagation*, Vol. 58, No. 12, 3821–3828, Dec. 2010.
11. Tong, K.-F. and T.-P. Wong, "Circularly polarized U-slot antenna," *IEEE Transactions on Antennas and Propagation*, Vol. 55, No. 8, 2382–2385, Aug. 2007.
12. Lam, K. Y., K.-M. Luk, K. F. Lee, H. Wong, and K. B. Ng., "Small circularly polarized U-slot wideband patch antenna," *IEEE Antenna Wireless Propag. Lett.*, Vol. 10, 87–90, 2011.
13. Heidari, A. A., M. Heyrani, and M. Nakhkash, "A dual-band circularly polarized stub loaded microstrip patch antenna for GPS applications," *Progress In Electromagnetics Research*, Vol. 92, 195–208, 2009.
14. Wang, C.-J. and C.-H. Lin, "A circularly polarized quasi-loop antenna," *Progress In Electromagnetics Research*, Vol. 84, 333–348, 2008.
15. Kasabegoudar, V. G. and K. J. Vinoy, "A broadband suspended microstrip antenna for circular polarization," *Progress*

In Electromagnetics Research, Vol. 90, 353–368, 2009.

16. Tiang, J.-J., M. T. Islam, N. Misram, and J. S. Mandeep, "Circular microstrip slot antenna for dual-frequency RFID application," *Progress In Electromagnetics Research*, Vol. 120, 499–512, 2011.
17. Sze, J.-Y. and S.-P. Pan, "Design of broadband circularly polarized square slot antenna with a compact size," *Progress In Electromagnetics Research*, Vol. 120, 513–533, 2011.
18. Yang, S. S., K.-F. Lee, A. A. Kishk, and K.-M. Luk, "Design and study of wideband single feed circularly polarized microstrip antennas," *Progress In Electromagnetics Research,* Vol. 80, 45–61, 2008.
19. Zarifi, D., H. Oraizi, and M. Soleimani, "Improved performance of circularly polarized antenna using semi-planar chiral metamaterial covers," *Progress In Electromagnetics Research*, Vol. 123, 337–354, 2012.
20. Herscovici, N., Z. Sipus, and D. Bonefacic, "Circularly polarized single-fed wide-band microstrip patch," *IEEE Transactions on Antennas and Propagation*, Vol. 51, No. 6, 1277–1280, Jun. 2003.
21. Chung, K. L. and A. S. Mohan, "A systematic design method to obtain broadband characteristics for singly-fed electromagnetically coupled patch antennas for circular polarization," *IEEE Transactions on Antennas and Propagation*, Vol. 51, No. 12, 3239–3248, Dec. 2003.
22. Sudha, T., T. S. Vedavathy, and N. Bhat, "Wideband single-fed circularly polarized patch antenna," *Electron. Lett.*, Vol. 40, No. 11, 648–649, May 2004.
23. Kim, S. M. and W. G. Yang, "Single feed wideband circular polarized patch antennam," *Electron. Lett.*, Vol. 43, No. 13, 703–704, Mar. 2007.
24. Wang, Z., S. Fang, S. Fu, and S. Jia, "Single-fed broadband circularly polarized stacked patch antenna with horizontally meandered strip for universal UHF RFID applications," *IEEE Trans. Microw. Theory Tech.*, Vol. 59, No. 4, 1066–1073, May 2011.
25. Shekhawat, S., P. Sekra, D. Bhatnagar, V. K. Saxena, and J. S. Saini, "Stacked arrangement of rectangular microstrip patches for circularly polarized broadband performance," *IEEE Antennas Wireless Propag. Lett.*, Vol. 9, 910–913, 2010.
26. Chen, X., G. Fu, S. X. Gong, et al., "A novel microstrip array antenna with coplanar parasitic elements for UHF RFID reader,"

Journal of Electromagnetic Waves and Applications, Vol. 23, Nos. 17–18, 2491–2502, 2009.

27. Chang, T. N. and J.-H. Jiang, "Enhance gain and bandwidth of circularly polarized microstrip patch antenna using gap-coupled method," *Progress In Electromagnetics Research*, Vol. 96, 127–139, 2009.
28. Sun, L., Y. L. Sun, and Y. H. Huang, "A novel wide band and broad beamwidth circularly polarized antenna," *Journal of Electromagnetic Waves and Applications*, Vol. 25, No. 10, 1459–1470, 2011.
29. Row, J.-S. and S.-W. Wu, "Circularly-polarized wide slot antenna loaded with a parasitic patch," *IEEE Transactions on Antennas and Propagation*, Vol. 56, No. 9, 2826–2832, Sep. 2008.
30. Han, T.-Y., Y.-Y. Chu, L.-Y. Tseng, and J.-S. Row, "Unidirectional circularly-polarized slot antennas with broadband operation," *IEEE Transactions on Antennas and Propagation*, Vol. 56, No. 6, 1777–1780, Jun. 2008.
31. Zhang, M. T, Y. B. Chen, and Y. C. Jiao, "Dual circularly polarized antenna of compact structure for RFID application," *Journal of Electromagnetic Waves and Applications*, Vol. 20, No. 14, 1895–1902, 2006.
32. Tsai, C. L., S. M. Deng, and C. H. Tseng, "Antennas with two shorted rectangular-ring slots coupled by microstrip line for the opposite sense CP in the wide-band operations," *Journal of Electromagnetic Waves and Applications*, Vol. 23, No. 10, 1367–1375, 2009.
33. Wang, A. N. and W. X. Zhang, "Design and optimization of broadband circularly polarized wide-slot antenna," *Journal of Electromagnetic Waves and Applications*, Vol. 23, No. 16, 2229–2236, 2009.
34. Row, J.-S., "The design of a squarer-ring slot antenna for circular polarization," *IEEE Transactions on Antennas and Propagation*, Vol. 53, No. 6, 1967–1972, Jun. 2005.
35. Tang, X., K.-L. Lau, Q. Xue, and Y. Long, "Design of small circularly polarized patch antenna," *IEEE Antennas Wireless Propag. Lett.*, Vol. 9, 728–731, 2010.
36. Wu, G.-L., W. Mu, G. Zhao, and Y.-C. Jiao, "A novel design of dual circularly polarized antenna fed by L-strip," *Progress In Electromagnetics Research*, Vol. 79, 39–46, 2008.
37. Ahdi Rezaeieh, S. and M. Kartal, "A new triple band circularly polarized square slot antenna design with crooked

T- and F-shaped strips for wireless applications," *Progress In Electromagnetics Research*, Vol. 121, 1–18, 2011.

38. Panda, J. R. and R. S. Kshetrimayum, "A printed 2.4 GHz/5.8 GHz dual-band monopole antenna with a protruding stub in the ground plane for WLAN and RFID Applications," *Progress In Electromagnetics Research*, Vol. 117, 425–434, 2011.
39. Bian, L., Y.-X. Guo, L. C. Ong, and X.-Q. Shi, "Wideband circularly-polarized patch antenna," *IEEE Transactions on Antennas and Propagation*, Vol. 54, No. 9, 2682–2686, Sep. 2006.
40. Guo, Y.-X., L. Bian, and X. Q. Shi, "Broadband circularly polarized annular-ring microstrip antenna," *IEEE Transactions on Antennas and Propagation*, Vol. 57, No. 8, 2474–2477, Aug. 2009.
41. Zhao, X., L. Zhao, and K. Huang, "A circularly polarized array composed of linear polarized microstrip patches fed by metamaterial transmission line," *Journal of Electromagnetic Waves and Applications*, Vol. 25, Nos. 11–12, 1545–1553, 2011.
42. Chen, X., G. Fu, S.-X. Gong, Y.-L. Yan, and W. Zhao, "Circularly polarized stacked annular-ring microstrip antenna with integrated feeding network for UHF RFID readers," *IEEE Antennas Wireless Propag. Lett.*, Vol. 9, 542–545, 2010.
43. Li, J.-F., B.-H. Sun, H.-J. Zhou, and Q.-Z. Liu, "Miniaturized circularly-polarized antenna using tapered meander-line structure," *Progress In Electromagnetics Research*, Vol. 78, 321–328, 2008.
44. Lau, P.-Y., K. K.-O. Yung, and E. K.-N. Yung, "A low-cost printed CP patch antenna for RFID smart bookshelf in library," *IEEE Trans. Industrial Electronics*, Vol. 57, No. 5, 1583–1588, May 2010.
45. Chen, X., G. Fu, S.-X. Gong, J. Chen, and X. Li, "A novel double-layer microstrip antenna array for UHF band RFID," *Journal of Electromagnetic Waves and Applications*, Vol. 23, Nos. 11–12, 1479–1487, 2009.
46. Liao, W.-J., S.-H. Chang, and Y. C. Chu, "A beam scanning phased array for UHF RFID readers with circularly polarized patches," *Journal of Electromagnetic Waves and Applications*, Vol. 24, Nos. 17–18, 2383–2395, 2010.
47. Invengo tags, "XC-TF8025-C02 Inlay," Shenzhen, China, 2012, http://www.invengo.cn/Products_show.asp?proid=973&classid=1&rsClass=6&threeID=31.